



RADIATION PARAMETERS OF THE PEAT BOG DUE TO PERMAFROST CONDITIONS VARIATIONS: A CASE STUDY OF THE OMA RIVER BASIN OF THE NENETS AUTONOMOUS OKRUG, NORTHWEST OF RUSSIA

Andrey V. Puchkov1*, Evgeny Yu. Yakovlev1

¹N. Laverov Federal Centre for Integrated Arctic Research of the Ural Branch of Russian Academy of Sciences, 109 Severnoj Dviny Emb., Arkhangelsk, 163000, Russia

*Corresponding author: andrey.puchkov@fciarctic.ru

Received: December 12nd 2024 / Accepted: June 19th 2025 / Published: October 1st 2025

https://doi.org/10.24057/2071-9388-2025-3762

ABSTRACT. The purpose of this article is to examine the distribution of natural radionuclides as well as the gamma radiation flux due to the variations of soil seasonal thawing depth. The study was conducted at a lumpy peat bog located within the catchment area of the Oma River, located within the Nenets Autonomous Okrug of Russia. The site was selected due to the presence of an active layer (AL) with varying depths of thawing, as well as the warming effect of the river. This feature enabled an initial assessment of the impact of thawing depth on radon flux, gamma radiation, and the distribution of other natural radionuclides along the peat profile. Field observations revealed that permafrost deposits act as a barrier to the intake of ²²²Rn from geological layers. The relationship between alterations in radiation parameters (gamma radiation flux, radon flux density (RFD), radionuclide composition of peat) and the thickness of the AL has been established. An increase in gamma radiation levels and RFD has been observed in areas exhibiting maximum seasonal thawing of the seasonally thawed layer. The correlation coefficients were found to be 0.70 and 0.83, respectively. The analysis of peat profiles in diverse permafrost settings revealed that in regions exhibiting deeper thawing of soil, there is an abundance of 210Pb relative to the concentration of its progenitor radionuclide, ²²⁶Ra. The observed excess of ²¹⁰Pb may be attributed to radon flux from deeper geological layers.

KEYWORDS: radon, permafrost, Arctic, climate warming, natural radioactivity, frozen soil, peat bog

CITATION: Puchkov A. V., Yakovlev E. Yu. (2025). Radiation Parameters Of The Peat Bog Due To Permafrost Conditions Variations: A Case Study Of The Oma River Basin Of The Nenets Autonomous Okrug, Northwest Of Russia. Geography, Environment, Sustainability, 3 (18), 32-42

https://doi.org/10.24057/2071-9388-2025-3762

ACKNOWLEDGEMENTS: This work was supported by the Ministry of Science and Higher Education of the Russian Federation (FUUW-2025-0011, project No. 125022002727-2).

Conflict of interests: The authors reported no potential conflict of interests.

INTRODUCTION

Permafrost plays an integral role in the Arctic natural environment, exerting a considerable influence on global change and human activity (Streletskiy et al. 2023). An increase in air temperature and snow cover parameters, particularly a reduction in snow depth, results in permafrost degradation, which is manifested as an expansion of the permafrost roof depth in both Arctic and mountainous regions (Streletskiy et al. 2023). It is observed that alterations in the boundaries of permafrost are occurring (Zhang et al. 2021). The consequences of permafrost degradation are already evident in several significant incidents, including the formation of extensive sinkholes in the Yamalo-Nenets Autonomous Okrug (Buldovicz et al. 2018) and the collapse of industrial facilities in Norilsk (Koptev 2020). Furthermore, permafrost can exert a considerable influence on the distribution of chemical elements in the environment.

Consequently, the degradation of permafrost may result in alterations to the chemical composition of the elements present, including radioactive elements, within soils and rocks (Shirokova et al. 2021; Pokrovsky et al. 2021; Puchkov et al. 2021).

Radon (²²²Rn) is a member of the radioactive 238U family and is ubiquitous in environmental components on Earth. 222Rn is continuously formed in all geological environments. The ²²²Rn decay sequence results in the emission of short-lived radioactive products, including ²¹⁸Po, ²¹⁴Pb, and ²¹⁴Bi, and long-lived ²¹⁰Pb and ²¹⁰Po, which are characterized by alpha and beta decay. The physical and chemical properties of ²²²Rn and its decay products permit its utilization as a tracer for the investigation of a multitude of geological and atmospheric processes (Sabbarese et al. 2021; Giustini et al. 2019; Miklyaev et al. 2010; Baskaran et al. 2016; Daraktchieva et al. 2021; Selvam et al. 2021). Concurrently, ²²²Rn and its decay products represent a

significant health risk, particularly in contexts where high concentrations are present, such as residential dwellings (Lorenzo-Gonzalez et al. 2020; Maier et al. 2021; Petrova et al. 2020; Rodríguez-Martínez et al. 2018; Rosenberger et al. 2018).

To date, there has been a paucity of scientific literature devoted to the behavior of ²²²Rn and its decay products in frozen rocks and permafros, while simultaneously observing the thawing and alteration of phase boundaries, which in turn modifies the pathways for ²²²Rn migration to the surface. The majority of these studies are of a theoretical nature (Puchkov et al. 2021). The results of the theoretical synthesis presented in Zhang et al. (2024) highlight the dearth of relevant studies on ²²²Rn migration and its relationship in permafrost regions, underscoring the urgent need for further research in this area. As the authors observe, priority research areas include the study of ²²²Rn migration mechanisms in freezing and thawing soils/rocks; the response to permafrost degradation due to the release of 222Rn absorbed in permafrost soils; and ²²²Rn migration in groundwater systems, among others. Scientists have published numerous articles on the experimental evaluation of ²²²Rn migration under conditions of varying temperatures (Puchkov 2022; Ye 2024). It has been demonstrated in existing scientific literature that permafrost serves as an effective barrier to the upward migration of ²²²Rn from the ground (Glover et al. 2022). This study highlights the necessity to extend these findings to other locations, given the heterogeneous and geographically distinctive nature of permafrost conditions. This prompts our investigation into the migration and flow of radioactive gases to the Earth's surface in the event of permafrost thawing.

The objective of this scientific article is to evaluate the flux of gamma radiation and RFD at the peat bog surface, as well as the distribution of natural radionuclides along the peat profile, under varying conditions of AL formation.

MATERIALS AND METHODS

Study area

The experimental site is situated in the Kanin tundra territory within the Nenets Autonomous Okrug in northwestern Russia (Fig. 2). The experimental site is the lumpy peat bog situated within the Oma River basin. Throughout the river basin, permafrost peat soils are prevalent. Soils of the alluvial soddy-gley and alluvialboggy types are present along the riverbanks. Alluvial solonchak soils are found at the river mouth. In the Kanin tundra territory (Chizha, Nes, Vizhas and Omariver basins), the average AL depth is up to 0.4 m, according to Iglovsky (2010). Average annual soil temperatures in the study area can range from +1.5 to -1.3°C in the AL and down to -3.5°C in the upper permafrost layers (Iglovsky 2010). The peat deposit is characterized by an uneven degree of decomposition. The upper layers (10–15 cm deep) contain highly decomposed peat (over 40%) mixed with the remains of shrubs, herbaceous plants, and lichens. The middle layer (10-30 cm) consists of poorly decomposed (5–10%) sphagnum peat. The lower layer consists of medium-decomposed (20–25%) sedge-sphagnum peat. The weight moisture content of peat can vary widely, from tens of percent in the upper, highly decomposed layers to 1000–2000% in the lower, weakly decomposed layers of the peat deposit (Prokhorenko 2013). Hillock peat ash content can range from 1.5 to 10%, peaking in the lower part of the AL. Closer to the mineral layer, the peat's ash content can increase to several tens of percent (Prokhorenko 2013).

The choice of the experimental site is conditioned by the varying thawing levels of AL, including the warming effect of the river. This peculiarity allows for an initial approximation of the influence of thawing depth on the ²²²Rn flux, gamma radiation, and the distribution of other natural radionuclides along the peat profile.

The methodology employed in the survey, along with the principal findings pertaining to the AL thaw depth, gamma radiation flux, and RFD estimation, are illustrated in Fig. 2. A total of 76 points were measured in the bog area, and two peat profile cuts were investigated. For gammaspectrometric measurements, peat and soil samples from two peat profile cuts were taken by shovel in a 20×20 cm plot at 5 cm horizons. Peat and soils in frozen condition were cut with a battery-powered electric saw. Sample preparation and measurements were carried out at the Environmental Radiology Laboratory of the Northern Laverov Federal Center for Integrated Arctic Research of the Ural Branch of the Russian Academy of Sciences (Russia, Arkhangelsk). The selected samples were allowed to dry in a BINDER E28 desiccator at 105°C. After drying, soil and peat samples were ashed at a temperature not exceeding 400°C to avoid loss of radionuclides. Ashing the soil and peat samples is necessary to improve the radionuclide detection efficiency of the semiconductor detector. This is done by reducing the volume and weight of the sample and the distance between the sample and the detector. The radionuclide activity presented in this paper is on a dry weight.

Radiometric measurement method

The measurement of the RFD utilizes the radon radiometer «Alpharad plus» (manufacturer: NTM Protection, Moscow city, Russia) (Fig. 1). The measurements were conducted in accordance with the prescribed algorithms and in compliance with the instructions set forth in the operational manuals. The equipment employs a semiconductor detector in which electrostatically charged ²¹⁸Po ions are deposited. The radiation parameters of ²²²Rn, including activity concentration and flux density, are determined by the number of registered alpha particles resulting from the decay of ²¹⁸Po atoms that fall on the detector (Afonin 2013).

Prior to the installation of the samplers, the soil surface was leveled and a 1 cm deepening was prepared. The sampler was left *in situ* for a period of 30 minutes, after which the air was pumped out of it into the measuring chamber of the radonometer. The measurements were conducted for a period of 20 minutes. In light of the necessity to perform a considerable number of RFD measurements, it was deemed appropriate to utilize two radon radiometers with identical technical specifications.

Gamma Spectrometry Measurements

Gamma spectrometry is a widely used method to measure gamma radiation from radionuclides of natural origin, including ²²⁶Ra. It is a universal, non-destructive and easy-to-use method, especially at the stage of sample preparation and in the measurement process (Syam et al. 2020). The radionuclides ²²⁶Ra, ²³²Th, ²¹⁰Pb, and 40K were determined using a low-background semiconductor gamma spectrometer manufactured by ORTEC (USA). The instrument is based on a coaxial detector, the GMX25, which is made of high-purity germanium (HPGe). The spectrometer is equipped with SpectraLine software. The relative efficiency of the gamma-ray spectrometer is 25%.

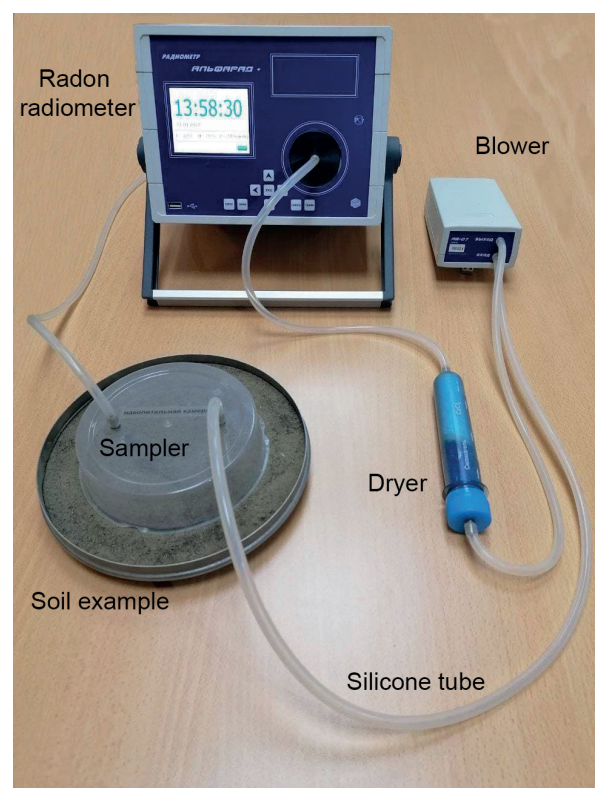


Fig. 1. The radon radiometer "Alpharad plus"

The calibration and quality control of gamma-spectrometric measurements were conducted using disc-type sources (OSGI-P) and special measures of volumetric activity, namely Marinelli beakers of varying density (RITWERZ, Russia-Germany). A plastic Petri dish with a diameter of 60 mm and a counting sample volume of 5 to 25 ml was chosen as the geometry for peat soil measurements. For clay bedrock samples, a 1-liter Marinelli vessel was used.

To achieve an equilibrium state of 226Ra decay products, the counting sample was sealed for a period of approximately three weeks. The Petri dishes were sealed using a sealant and duct tape. The samples were measured for a minimum of 12,000 seconds. The primary gammaray energies of ²¹⁴Pb (351.93 keV) and ²¹⁴Bi (609.32 keV, 1120.29 keV, 1764.49 keV) were employed to detect ²²⁶Ra and ascertain its activity concentration. The primary gamma-ray energies of ²¹²Pb (238.63 keV), ²²⁸Ac (911.20 keV) and ²⁰⁸Tl (583.19 keV, 2614.51 keV) were employed to identify ²³²Th and quantify its activity concentration. In this study, it was assumed that the decay products of ²³²Th and the parent radionuclide itself are in a state of radioactive equilibrium. The activity concentration of the radionuclide ²¹⁰Pb was determined from the 46.50 keV gamma ray line, while the activity concentration of radionuclide 40K was determined using the energy of 1460.82 keV.

Dosimetry measurements

To measure gamma radiation flux, the scintillation geological exploration radiometer SRP-88n was employed. The measurements were conducted in accordance with the prescribed algorithms and in compliance with the instructions set forth in the operational manuals. The height of the measurements at each point was 10 cm.

AL thaw level measurements

AL thawing level measurements were carried out using a contact thermometer TK-5.04 with a submersible probe of length L=500 mm. At each control point, the

probe was immersed into the ground as far as it would go in at least 3 locations 10 cm apart. This method was used to exclude the probe stop in hard material (stone, wood). The parameter that indicated the level of ice in the ground was the probe temperature = 0 degrees Celsius. The level of ground thawing was measured by the depth of probe immersion. The average value of at least 3 immersions into the ground up to the ice stop was taken as the result.

Quality control of measurements

The determination of ²²²Rn, ²²⁶Ra, ²³²Th, 40K, ²¹⁰Pb, and gamma ray flux was conducted utilizing the instrumentation of the Environmental Radiology Laboratory of the N. Laverov Federal Center for Integrated Arctic Research of the Ural Branch of the Russian Academy of Sciences (Russia, Arkhangelsk), which is in compliance with the accreditation criteria for testing laboratories as outlined in ISO/IEC 17025. The laboratory is equipped with an extensive range of reference radionuclide sources, which are employed for the calibration of equipment and the monitoring of measurement quality.

If the measurement result was beyond the sensitivity of the measuring instrument, parallel measurements were made at such points. The result was accepted if the following condition was fulfilled (Eq. 1):

$$\left|A_{1}-A_{2}\right|<\sqrt{\delta A_{1}^{2}+\delta A_{2}^{2}}\tag{1}$$

where A_1 and A_2 – measurement results; $\delta A_{1,2}$ – uncertainties of measurement results A_1 and A_2 .

If the condition was not fulfilled, the measurement was repeated again.

Statistical analysis

Statistical analysis was performed using licensed software packages OriginPro and Microsoft Office. Mapping was carried out using Surfer software by Golden Software, Inc. (Golden, Colorado, USA).

RESULTS

The study scheme and the main results of AL thaw depth, gamma ray flux, and RFD are summarized in Fig. 2.

During the study period (July 2023), the greatest depth of AL thawing was observed along the edge of the bog (band width not exceeding 1-2 m), reaching 50-60 cm (bedrock level). From the edge of the bog, the thawing depth decreased markedly, with a range of 5 to 15 cm.

The gamma radiation flux within the area under study exhibits a range of 14.4 to 30.4 impulses per second, with an average value of 21.7 impulses per second. The results of the measurements indicated a slight increase in gamma ray flux in areas of maximum AL thawing within the peat strata. A comparable distribution pattern is evident for RFD in the area under study. The parameter in question exhibits a range of 6.0 to 44.0 mBq·m-²·s-¹, with an average value of 16.4 mBq·m-²·s-¹. The highest RFD values are observed along the edge of the peat bog, within a band with a width of no more than 1-2 m.

Two peat profile cuts were conducted within the bog, one at the edge (Profile 1) and one at a distance of 100 meters (Profile 2) (Fig. 3). The results of the assessment of the natural radionuclide content in samples from peat profile cuts are presented in Tables 1 and 2.

For the purposes of clarity and informative content, the results presented in Tables 1 and 2 are plotted in Fig. 4. As evidenced in Tables 1 and 2, the distribution of radionuclides ²²⁶Ra, ²¹⁰Pb, ²³²Th, and 40K exhibits a comparable pattern across the depth of peat profile cuts. In general, the values of these radionuclides are consistent with the available data for the Northwest region, as reported by Kriauciunas (2018), Yakovlev (2022, 2023).

The ²¹⁰Pb activity concentration ranges from the lowest measured values (2.3±1.1 Bq·kg⁻¹ for the 20-25 cm horizon) to 330.0±60.0Bq·kg⁻¹forpeatprofile1andfromthelowestmeasured values (4.1±1.9 Bq·kg⁻¹ for the 15-20 cm horizon) to 270.0±60.0 Bq·kg⁻¹ for peat profile 2. The maximum activity concentration of ²¹⁰Pb (330.0±60.0 Bq·kg⁻¹) falls on the uppermost horizon (0-5 cm), which is a natural phenomenon given that the

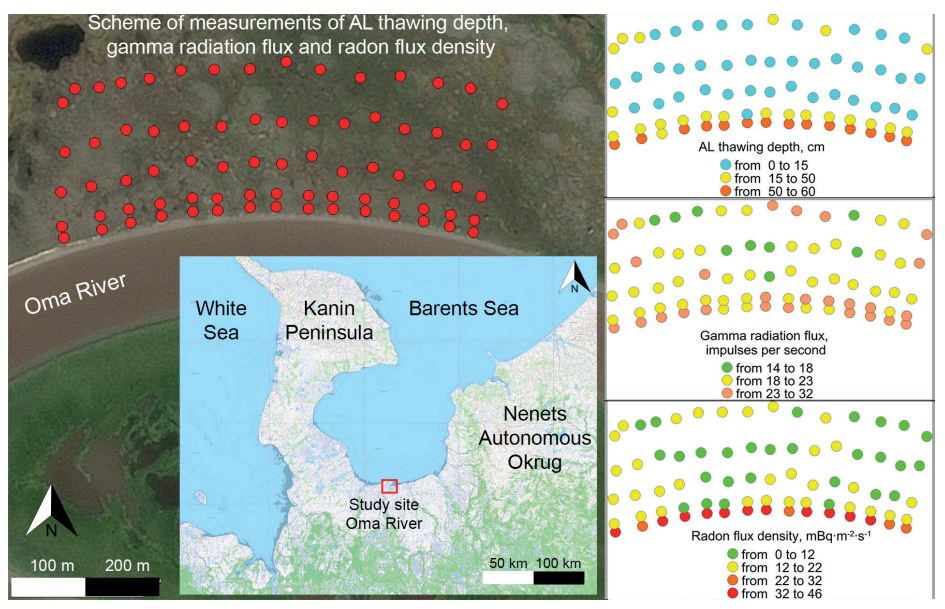


Fig. 2. Distribution of gamma ray flux, RFD over peat bog surface, and AL thawing depth in the Oma River basin

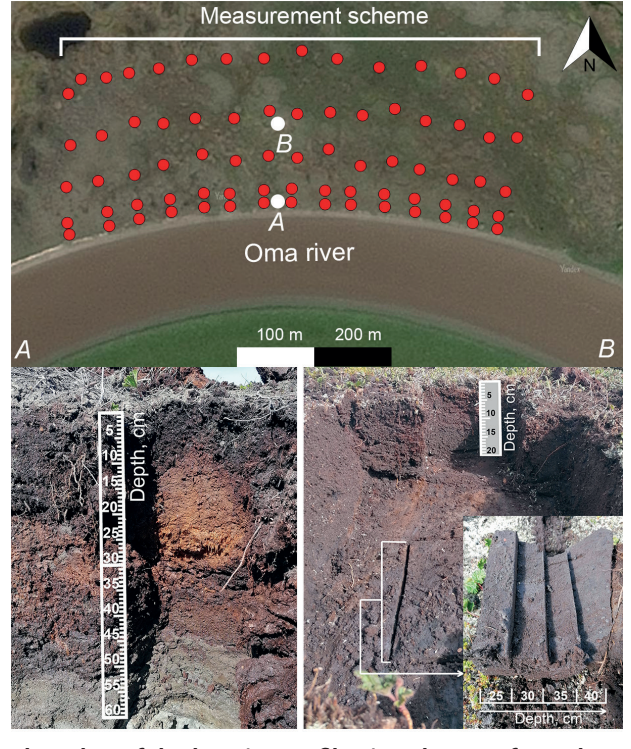


Fig. 3. Peat profile cuts at the edge of the bog (A, profile 1) and 100 m from the edge of the bog (B, profile 2)

Table 1. Variation of natural radionuclide content with depth in profile 1

Layer, cm	Activity concentration, Bq·kg ⁻¹				Isotopic ratio
	²²⁶ Ra	²¹⁰ Pb	²³² Th	40K	²²⁶ Ra/ ²¹⁰ Pb
0-5	< MDA	330.0±60.0	3.1±1.0	60.0±18.0	-
5-10	< MDA	65.0±18.2	2.5±1.0	51.0±19.0	-
10-15	< MDA	10.0±2.5	2.0±0.8	45.0±18.0	-
15-20	< MDA	< MDA	< MDA	35.0±14.0	-
20-25	0.3±0.2	2.3±1.1	1.3±0.8	23.0±9.2	0.13
25-30	1.1±0.4	8.1±3.2	4.8±0.6	78.0±12.5	0.14
30-35	2.8±0.8	7.3±2.9	4.5±0.6	62.0±11.8	0.38
35-40	2.3±0.7	12.0±5.0	5.1±0.7	155.0±21.7	0.19
40-45	10.5±1.6	16.0±6.4	20.1±1.8	330.0±29.7	0.66
45-50	14.2±2.6	21.0±8.4	25.0±2.3	370.0±33.3	0.68
50-55	16.3±2.5	17.0±6.8	25.9±2.2	530.0±47.7	0.96

Table 2. Variation of natural radionuclide content with depth in profile 2

Layer, cm	Activity concentration, Bq·kg ⁻¹				Isotopic ratio
	²²⁶ Ra	²¹⁰ Pb	²³² Th	40K	²²⁶ Ra/ ²¹⁰ Pb
0-5	< MDA	270.0±60.0	< MDA	51.0±18.0	-
5-10	< MDA	22.0±18.2	< MDA	45.0±19.0	-
10-15	< MDA	< MDA	< MDA	35.0±18.0	-
15-20	< MDA	4.1±1.9	4.8±2.3	78.0±14.0	-
20-25	3.6±0.2	9.0±1.1	8.6±0.8	155.0±9.2	0.40
25-30	3.3±0.4	6.5±3.2	8.4±0.6	183.0±12.5	0.51
30-35	4.5±0.8	11.0±2.9	9.6±0.6	167.0±11.8	0.41
35-40	5.8±0.7	8.0±5.0	9.7±0.7	190.0±21.7	0.73

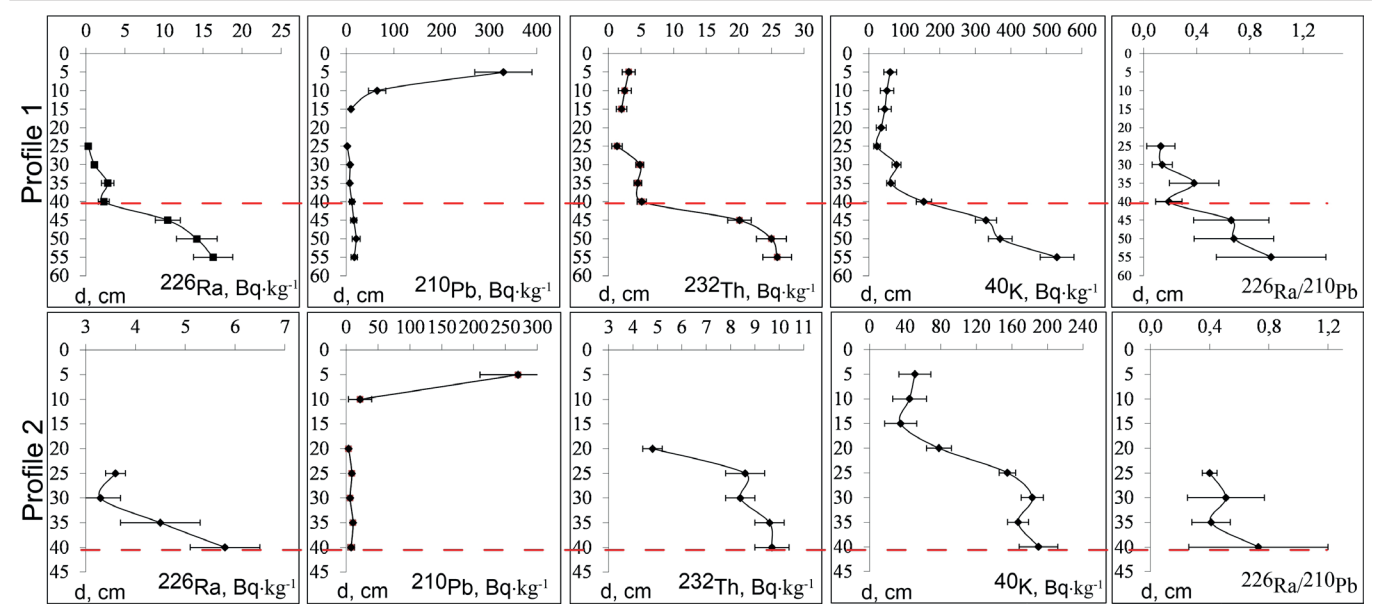


Fig. 4. Plots of radionuclide activity concentration distribution and isotopic ratios along profiles 1 and 2 (red dashed line shows average AL level according to (Iglovsky 2010))

only way ²¹⁰Pb enters the peatland is atmospheric fallout (Yakovlev et al. 2022). The concentration of 210Pb at a depth of 15-20 cm in profile 1 and 10-15 cm in profile 2 is below the minimum detectable activity concentration. In general, the ²¹⁰Pb activity concentration in the studied profiles is comparable to other regions of Northwest Russia. For instance, the maximum ²¹⁰Pb activity concentration recorded in the Ilassky peatland in the Arkhangelsk region was 310.8 Bq·kg⁻¹ (Yakovlev et al. 2022). However, there are cases where the vertical distribution of ${\rm ^{210}Pb}$ differs from the above. Cwanek and Łokas (2022) demonstrated that the highest activity concentration was not confined to the uppermost layer but occurred within intermediate depths. Additionally, there were significant deviations from the simple monotonic decrease of atmospheric components, which often fluctuated downward, presumably reflecting episodic variations in recent peat growth or decomposition

The vertical distribution of ²²⁶Ra, ²³²Th, and 40K differs from the vertical distribution of ²¹⁰Pb for our study area. The maximum values of these radionuclides are observed in the underlying horizons. This effect is especially noticeable for peat profile 1, where samples were taken including the bedrock, with increased sorption properties of clay minerals.

DISCUSSION

The obtained data sets of AL, RFD and gamma flux density differ from the normal distribution, so we used the nonparametric Spearman's rank criterion to evaluate correlation dependencies. A correlation coefficient of 0.70 (significant at the 0.05 p-value) was observed between gamma ray flux and AL thawing depth. It is likely that the elevated gamma ray flux is attributable to the flux of natural radioactive gases, including ²²²Rn and its decay products, given the absence of a permafrost barrier. Conversely, the observed increase in gamma radiation flux may be attributed to intrinsic properties of gamma radiation. The ability of gamma radiation to penetrate an object is contingent upon the energy of the gamma quantum and the density of the substance absorbing it. The thickness of the water layer at 24 cm (which, in the present study, is equated with the thickness of the frozen ground) attenuates the gamma radiation flux with an energy of 0.5 MeV by a factor of 10. Given the considerable range of gamma-radiation energies exhibited by natural radionuclides (Levin 1973), spanning from the X-ray zone to energies exceeding 2.5 MeV, ice or frozen ground can serve as a substantial barrier to the passage of gammaquanta. This phenomenon may be reflected in the findings of studies examining the distribution of gamma-ray flux in peat bogs within the Oma River basin.

In contrast to gamma radiation, there is a very strong correlation between RFD and the AL thaw level of 0.83 (significant at the 0.05 *p-value*). Concurrently, a comparison of RFD and gamma radiation flux reveals a relatively weak correlation between these parameters – 0.59 (significant at the 0.05 *p-value*)). It can be reasonably assumed that the greatest contribution to the gamma-quantum flux is made by gamma-emitting radionuclides, including ²²²Rn decay products present in the soil. ⁴⁰K, a radionuclide found in abundance in natural environments, also emits gamma radiation. In the present study, its activity concentration exceeds that of other radionuclides, especially in the underlying horizons. Furthermore, the gamma-ray energy of ⁴⁰K is notably high at 1460 keV. However, it is important to note that the beta decay of ⁴⁰K is accompanied by

gamma-quantum yield in only 10.6% of cases (Levin 1973). Consequently, the contribution of 40K to the total gamma radiation flux is likely to be approximately equivalent to that of other radionuclides.

The surface distribution of radiation parameters can be directly related to the vertical distribution of radionuclides in different frozen conditions. As previously mentioned, the concentration of 210Pb at a depth of 15-20 cm in profile 1 and 10-15 cm in profile 2 is below the minimum detectable activity concentration. This lower concentration is likely attributable to the absence of vertical migration of ²¹⁰Pb, which entered via atmospheric deposition due to the shallow depth of the AL and its brief melt period. Conversely, in horizons deeper than 15-20 cm, both profiles demonstrate an increase in the content of ²¹⁰Pb, as well as its parent isotope ²²⁶Ra. The results of the calculation of the ²²⁶Ra/²¹⁰Pb isotopic ratio for depths between 20 and 40 cm demonstrated that in profile 1, this parameter exhibited a range of 0.13 to 0.38, while in profile 2, it varied between 0.40 and 0.73. The low value of the isotopic ratio in profile 1 may be indicative of an excess of ²¹⁰Pb (in comparison to the ²²⁶Ra content), which is likely due to the ²²²Rn flux from the underlying horizons. The application of the ²²⁶Ra/²¹⁰Pb isotope ratio method is discussed in detail by Tsapalov (2013). The authors demonstrate that the ²¹⁰Pb content is excessive in conditions of active geodynamics due to the inflow of «deep» ²²²Rn. In the present study, it is hypothesized that in permafrost conditions, the activities of ²²⁶Ra and ²¹⁰Pb are in radioactive equilibrium, whereby their ratio is assumed to be 1 (one). This assumption is founded upon a series of indirect indications, as direct evidence for this phenomenon is not available within the scientific literature. For instance, in 1990, research was conducted to assess the distribution of permafrost by measuring the activity concentration of ²²²Rn as a tracer (Sellmann et al. 1990). The results of the studies demonstrated a strong correlation between the ²²²Rn activity concentration and frozen areas in the permafrost distribution, with varying levels of permafrost roof occurrence. The necessity to take into account the factors such as surface ice and permafrost presence when assessing ²²²Rn distribution was pointed out in Evangelista et al. (2002). It has been hypothesised that surface ice and permafrost act as significant barriers to the ²²²Rn flux reaching the Earth's surface. Theoretical studies on this contentious issue were initiated in 2006-2008 (Glover 2022). Conclusions have been drawn by Russian scientists (Klimshin et al. 2010) regarding the significant influence of the level of seasonal ground freezing (up to 1 m) in wintertime on ²²²Rn emanation to the Earth's surface. The evidence suggests that 222Rn may be sealed within the permafrost. The absence of ²²²Rn migration can be interpreted as an absence of both ²²²Rn itself and its decay products. However, when permafrost conditions are disrupted, ²²²Rn will begin to migrate through the geological environment (Puchkov et al. 2021), leaving behind radioactive decay products, which may potentially result in a reduction in the value of the ²²⁶Ra/²¹⁰Pb ratio.

In terms of the ongoing discussion of ²²⁶Ra/²¹⁰Pb ratio violations, there is a further potential cause of the ²¹⁰Pb excess: the compression of pore waters and gases (including gas hydrates) containing ²²²Rn because of cryogenic concentration from the permafrost zone to the freezing zone (Chuvilin et al. 2000). The ²²²Rn does not form gas hydrate crystals with water independently, as it lacks the requisite partial pressure for hydrate formation. However, its atoms are actively embedded in the nodes of hydrate crystals of the auxiliary gas, thereby forming a mixed hydrate (Portman 2014).

It is important to note that the discussions presented above do not conclusively address the issues of increased ²²²Rn fluxes resulting from permafrost degradation and the deterioration of the radiological situation in areas with an unfavorable radiochemical background. These issues remain open for further debate and investigation. The results of the observed increase in ²²²Rn and gamma radiation fluxes can be interpreted not only in the context of permafrost conditions but also in relation to other factors. The measured RFD values indicate that the concentration of ${}^{222}\!Rn$ decay daughter products in the air and on the soil surface is likely insufficient to significantly impact gamma radiation flux values. To this end, it would be advisable to conduct a further study in territories with an unfavorable radiogeochemical background. The excess of ²¹⁰Pb compared to ²²⁶Ra may be related to the increased concentration of ²¹⁰Pb in this layer. This level is probably formed in autumn and early winter during freezing of the AL from above. In this process, soil ²²²Rn cannot escape to the atmosphere and appears 'sealed' in the melted area between permafrost rocks and the freezing layer. For example, Klimshin et al. (2010) demonstrate that the freezing of the surface soil layer can reduce the ²²²Rn flux by up to 10 times compared to the period preceding freezing.

CONCLUSIONS

This paper presents the findings of field studies investigating the distribution of ²²⁶Ra, ²²²Rn, its decay products, and gamma radiation flux in relation to varying levels of AL occurrence. The studies were conducted on the territory of a hillocky peat bog situated within the Oma River basin, which is located in the Nenets Autonomous

Okrug in Russia. A total of 76 points were sampled across the bog territory, and two peat profile cuts were investigated.

A significant correlation has been revealed between the gamma radiation flux and AL, which may be related, on the one hand, to the flux of natural radioactive gases and accumulation of their decay products in the absence of a frozen barrier. This hypothesis is further substantiated by the substantial correlation between RFD and AL (R = 0.83). Conversely, the association between gamma radiation and AL may be attributable to inherent characteristics of gamma radiation itself.

The vertical migration of natural radionuclides ²¹⁰Pb, ²²⁶Ra, ²³²Th, and ⁴⁰K was studied in two selected peat profile cuts. The highest activity concentration of ²¹⁰Pb is observed in the upper peat horizon (330.0±60.0 Bq·kg⁻¹ for profile 1 and 270.0±60.0 Bq·kg⁻¹ for profile 2), which is associated with atmospheric deposition. The ²¹⁰Pb activity concentration sharply decreases to the minimum detectable values in the 10-20 cm horizon, which may be related to the absence of vertical migration of atmospheric ²¹⁰Pb as a result of permafrost spreading and short AL thawing periods. In the underlying horizons of profile 1, where the AL thawing level is the highest, a violation of the ²²⁶Ra/²¹⁰Pb isotopic ratio is noted in favor of a ²¹⁰Pb increase. We attribute this fact to the increased flux of ²²²Rn from the underlying horizons in the absence of a permafrost barrier. However, we do not exclude other possible factors of ²¹⁰Pb excess in the underlying horizons under permafrost thawing conditions, such as the compression of pore waters and gases (including gas hydrates) containing ²²²Rn because of cryogenic concentration from the permafrost zone to the freezing zone.

REFERENCES

Afonin A. and Korchunov A. (2013). Optimizing block parameters measurements for monitoring radon, thoron and their daughter products in various environments. ANRI, 1, 9-11. (in Russian).

Baskaran M. (2016). Radon: A tracer for geological, geophysical and geochemical studies. Basel: Springer, DOI: 10.1007/978-3-319-21329-3.

Buldovicz S. N., Khilimonyuk V. Z., Bychkov A. Y., Ospennikov E. N., Vorobyev S. A., Gunar A. Y., Gorshkov E. I., Chuvilin E. M., Cherbunina M. Y., Kotov P. I., Lubnina N. V., Motenko R. G. and Amanzhurov R. M. (2018). Cryovolcanism on the Earth: Origin of a Spectacular Crater in the Yamal Peninsula (Russia). Scientific Reports, 8(1), DOI: 10.1038/s41598-018-31858-9.

Chuvilin E.M., Yakushev V.Sand Perlova E.V. (2000). Gas and gas hydrates in the permafrost of Bovanenkovo gas fi eld, Yamal Peninsula, West Siberia. Polarforschung, 68, 215-219.

Cwanek A. and Łokas E. (2022). Deposition chronologies in a peat bog from Spitsbergen (High Arctic) using the 210Pb dating method. Polish Polar Research, 43(4), DOI: 10.24425/ppr.2022.143310.

Daraktchieva Z., Wasikiewicz J. M., Howarth C. B. and Miller C. A. (2021). Study of baseline radon levels in the context of a shale gas development. Science of The Total Environment, 753, 141952, DOI: 10.1016/j.scitotenv.2020.141952.

Evangelista H. and Pereira, E. B. (2002). Radon flux at King George Island, Antarctic Peninsula. Journal of Environmental Radioactivity, 61(3), DOI: 10.1016/S0265-931X(01)00137-0.

Giustini F., Ciotoli G., Rinaldini A., Ruggiero L. and Voltaggio M. (2019). Mapping the geogenic radon potential and radon risk by using Empirical Bayesian Kriging regression: A case study from a volcanic area of central Italy. Science of the Total Environment, 661, 449-464, DOI: 10.1016/j.scitotenv.2019.01.146.

Glover P. W. J. and Blouin, M. (2022). Increased Radon Exposure From Thawing of Permafrost Due To Climate Change. Earth's Future, 10(2), DOI: 10.1029/2021EF002598.

Iglovsky S. A., Shvartsman Y. G. and Bolotov I. N. (2010). Cryolithozone of the Dvinsko-Mezenskaya Plain and Kanin Peninsula. Ekaterinburg: FCIARCTIC UrB RAS (in Russian).

Klimshin A.V., Kozlova I.A., Rybakov E.N. and Lukovskoy M.Yu. (2010). Effect of freezing the surface layer of soil on the radon transport. KRAUNTS Bulletin. Series: Earth Sciences, 16(2), 146-151 (in Russian with English summary).

Koptev D.P. (2020). Norilsk spill: lessons and consequences. Drilling and Oil, (7-8), 3-9. (in Russian with English summary).

Kriauciunas V. V., Iglovsky S. A., Kuznetsova I. A., Shakhova E. V., Bazhenov A. V. and Mironenko K. A. (2018). Spatial distribution of natural and anthropogenic radionuclides in the soils of Naryan–Mar. Arctic Environmental Research, 18 (3), 82-89, DOI: 10.3897/issn2541–8416.2018.18.3.82.

Levin V. E. and Khamyanov L. P. (1973). Registration of ionising radiation. Moscow: Atomizdat. (in Russian).

Lorenzo-Gonzalez M., Ruano-Ravina A., Torres-Duran M., Kelsey K. T., Provencio M., Parente-Lamelas I., Piñeiro-Lamas M., Varela-Lema L., Perez-Rios M., Fernandez-Villar A. and Barros-Dios J. M. (2020). Lung cancer risk and residential radon exposure: A pooling of case-control studies in northwestern Spain. Environmental Research, 189, DOI: 10.1016/j.envres.2020.109968.

Maier A., Wiedemann J., Rapp F., Papenfuß F., Rödel F., Hehlgans S., Gaipl U. S., Kraft G., Fournier C. and Frey B. (2021). Radon exposure-therapeutic effect and cancer risk. International Journal of Molecular Sciences, 22(1), DOI: 10.3390/ijms22010316.

Miklyaev P. S. and Petrova T. B. (2010). The study of radon emanation in clay. Geoecology. Engineering geology, hydrogeology, geocryology, (1), 13-22, (in Russian).

Petrova T. and Miklyaev P. (2020). Variations of indoor radon concentration in traditional russian rural wooden houses. Radiation Protection Dosimetry, 191(2), DOI: 10.1093/rpd/ncaa156.

Pokrovsky O. S., Manasypov R. M., Pavlova O. A., Shirokova, L. S. and Vorobyev S. N. (2022). Carbon, nutrient and metal controls on phytoplankton concentration and biodiversity in thermokarst lakes of latitudinal gradient from isolated to continuous permafrost. Science of the Total Environment, 806, DOI: 10.1016/j.scitotenv.2021.151250.

Portman A. I. and Potemkin A. M. (2014). Gas-hydrate method of radon immobilisation ANRI, 4(79), 61-64 (in Russian).

Prokhorenko N. B. (2013). Classification and composition of peat. Kazan: Kazan (Volga Region) Federal University (in Russian).

Puchkov A. V., Berezina E. V., Yakovlev E. Y., Hasson N. R., Druzhinin S. V., Tyshov A. S., Ushakova E. V., Koshelev L. S. and Lapikov P. I. (2022). Radon Flux Density In Conditions Of Permafrost Thawing: Simulation Experiment. Geography, Environment, Sustainability, 15(3), DOI: 10.24057/2071-9388-2022-023.

Puchkov A. V., Yakovlev E. Y., Hasson N., Sobrinho G. A. N., Tsykareva Y. V., Tyshov A. S., Lapikov P. I. and Ushakova E. V. (2021). Radon Hazard In Permafrost Conditions: Current State Of Research. Geography, Environment, Sustainability, 14(4), DOI: 10.24057/2071-9388-2021-037.

Rodríguez-Martínez Á., Torres-Durán M., Barros-Dios J. M. and Ruano-Ravina, A. (2018). Residential radon and small cell lung cancer. A systematic review. In Cancer Letters, 426, DOI: 10.1016/j.canlet.2018.04.003

Rosenberger A., Hung R. J., Christiani D. C., Caporaso N. E., Liu G., Bojesen S. E., le Marchand L., Haiman C. A., Albanes D., Aldrich M. C., Tardon A., Fernández-Tardón G., Rennert G., Field J. K., Kiemeney B., Lazarus P., Haugen A., Zienolddiny S., Lam S. and Gomolka M. (2018). Genetic modifiers of radon-induced lung cancer risk: a genome-wide interaction study in former uranium miners. International Archives of Occupational and Environmental Health, 91(8), DOI: 10.1007/s00420-018-1334-3.

Sabbarese C., Ambrosino F., D'Onofrio A., Pugliese M., La Verde G., D'Avino V. and Roca V. (2021). The first radon potential map of the Campania region (southern Italy). Applied Geochemistry, 126, 104890, DOI:10.1016/j.apgeochem.2021.104890.

Sellmann P. V. and Delaney A. J. (1990). Radon measurements as indicators of permafrost distribution. Cold Regions Science and Technology, 18(3), DOI: 10.1016/0165-232X(90)90029-V.

Selvam S., Muthukumar P., Sajeev S., Venkatramanan S., Chung S. Y., Brindha K. and Murugan R. (2021). Quantification of submarine groundwater discharge (SGD) using radon, radium tracers and nutrient inputs in Punnakayal, south coast of India. Geoscience Frontiers, 12(1), 29-38, DOI: 10.1016/j.gsf.2020.06.012.

Shirokova L. S., Chupakov A. V., Ivanova I. S., Moreva O. Y., Zabelina S. A., Shutskiy N. A., Loiko S. V. and Pokrovsky O. S. (2021). Lichen, moss and peat control of C, nutrient and trace metal regime in lakes of permafrost peatlands. Science of the Total Environment, 782, DOI: 10.1016/j. scitotenv.2021.146737

Streletskiy D. A., Clemens S., Lanckman J. P. and Shiklomanov N. I. (2023). The costs of Arctic infrastructure damages due to permafrost degradation. Environmental Research Letters, 18(1), DOI: 10.1088/1748-9326/acab18.

Syam N. S., Lim S., Lee H. Y. and Lee, S. H. (2020). Determination of radon leakage from sample container for gamma spectrometry measurement of 226Ra. Journal of environmental radioactivity, 220, 106275, DOI: 10.1016/j.jenvrad.2020.106275

Tsapalov A. A., Miklyaev P. S. and Petrova T. B. (2013). The principle of detection of sites with active geodynamics based on the analysis of the ratio of Pb-210/Ra-226 activities in soil samples. ANRI, 1(72).

Yakovlev E., Orlov A., Kudryavtseva A. and Zykov S. (2022). Estimation of Physicochemical Parameters and Vertical Migration of Atmospheric Radionuclides in a Raised Peat Bog in the Arctic Zone of Russia. Applied Sciences (Switzerland), 12(21), DOI: 10.3390/app122110870.

Yakovlev E., Orlov A., Kudryavtseva A., Zykov S. and Zubov I. (2023). Assessment of the Impact of Anthropogenic Drainage of Raised Peat-Bog on Changing the Physicochemical Parameters and Migration of Atmospheric Fallout Radioisotopes in Russia's Subarctic Zone (Subarctic Zone of Russia). Applied Sciences (Switzerland), 13(9), DOI: 10.3390/app13095778.

Ye Y., Wang H., Li M. and Chen M. (2024). Experimental study of radon migration parameters in uranium tailings under frozen and non-frozen conditions. Journal of Radioanalytical and Nuclear Chemistry, 334, 439-447, DOI: 10.1007/s10967-024-09842-7.

Zhang S., Jin D., Jin H., Li C., Zhang H., Jin X. and Cui J. (2024). Potential radon risk in permafrost regions of the Northern Hemisphere under climate change: A review. In Earth-Science Reviews, 250, DOI: 10.1016/j.earscirev.2024.104684.

Zhang Z. Q., Wu Q. B., Hou M. T., Tai B. W. and An Y. K. (2021). Permafrost change in Northeast China in the 1950s–2010s. Advances in Climate Change Research, 12(1), DOI: 10.1016/j.accre.2021.01.006.

APPENDIX A Table A1. RFD, AL, and gamma radiation flux at the peat bog surface

ID point	RFD*, mBq·m ⁻² ·s ⁻¹	AL, cm	Gamma radiation flux*, impulses per second
1	30	53	25.9
2	25	52	25.8
3	29	49	29.7
4	36	50	27.9
5	32	55	23.7
6	31	50	21.9
7	35	51	22.1
8	29	54	23.8
9	28	59	26.2
10	31	50	18.3
11	36	51	20.3
12	37	54	25.9
13	32	53	24.7
14	25	55	30.4
15	26	56	28.6
16	18	14	19.9
17	10	7	18.3
18	11	8	19.6
19	12	8	22.0
20	11	10	18.4
21	15	9	21.8
22	14	9	18.5
23	16	8	16.0
24	9	10	18.0
25	9	12	18.3
26	10	12	16.3
27	12	8	22.7
28	12	9	20.1
29	14	13	18.1
30	15	15	20.3
31	14	12	22.1
32	13	11	23.7
33	10	12	22.3
34	6	11	21.4
35	7	9	20.6

36	9	9	15.9
37	10	8	17.7
38	8	9	17.9
39	6	10	18.4
40	15	12	20.6
41	16	12	21.9
42	11	11	16.3
43	6	12	20.4
44	8	10	18.1
45	7	13	23.9
46	19	44	25.7
47	8	12	21.6
48	10	13	19.7
49	11	10	16.8
50	14	33	23.4
51	11	14	23.6
52	19	39	25.3
53	16	12	22.7
54	15	12	18.5
55	12	11	14.6
56	13	10	16.2
57	9	10	14.4
58	10	28	20.3
59	21	47	23.9
60	21	48	24.3
61	18	24	19.0
62	24	30	21.9
63	18	29	26.3
64	19	28	22.7
65	20	32	22.1
66	20	49	32.1
67	24	20	18.2
68	23	41	23.0
69	24	39	26.5
70	23	42	23.0
71	19	37	18.6
72	20	45	22.3
73	21	44	26.8

74	20	29	22.1
75	23	26	24.9

^{*}Notes: According to the technical documentation, the uncertainty of measurements with the scintillation geological exploration radiometer SRP-88n is 10%. According to the technical documentation, the uncertainty of measurements with the radon radiometer «Alpharad plus» is 30%.